

Local Hybrid Functionals

Juanita Jaramillo and Gustavo E. Scuseria
Department of Chemistry, Rice University, Houston, TX 77005-1892, USA

Matthias Ernzerhof
*Département de Chimie, Université de Montréal, Montréal, Québec, Canada H3C 3J7**
(Dated: October 30, 2002)

We present a novel approach for constructing hybrid functionals by using a local mix of regular density functional theory (DFT) exchange and exact Hartree-Fock (HF) exchange. This local hybrid approach is computationally feasible for a wide range of molecules. In this work, the local mix of HF and DFT exchange is driven by the ratio of $\tau_W = \frac{|\nabla\rho|^2}{8\rho}$, the Weizsäcker kinetic energy density, with τ , the exact kinetic energy density. This particular choice of local mix yields 100% of exact exchange in one-electron regions. Dissociation energy curves, binding energies, and equilibrium geometries for two-center three-electron symmetric radical cations can be modeled accurately using this scheme. We also report encouraging results for reaction energy barriers, and somewhat disappointing atomization energies for the small G2 set.

I. INTRODUCTION

Density functional theory (DFT) [1] is a very successful model for studying chemical systems. DFT predicts thermochemical and structural properties with accuracy similar to conventional correlated *ab initio* methods such as second order perturbation theory (MP2) when compared to experimental data. This is achieved even though DFT is computationally more cost-effective [2] than MP2.

Hybrid functionals are the most popular class of functionals for molecules because of their improved results over local density approximation (LSDA) and generalized gradient approximations (GGA) for molecular thermochemistry and structural calculations. Hybrid methods include a fixed combination of conventional DFT and exact Hartree-Fock exchange with a small added computational cost. Traditionally, 20 to 25% of exact HF exchange is included in hybrid methods [3, 4]. However, multiple examples of the failure of this type of mixing [5] show that an excess or deficiency of exact exchange is present for some systems. Ideally, the mixing coefficient should be determined according to the properties of each system [6].

Despite the wide success of approximate density functional theory, current functionals exhibit problems when modelling certain type of systems. Problematic situations include radicals, reaction energy barriers, charge transfer complexes, Rydberg excited states, and van der Waals interactions. Some of these difficulties arise in part as a consequence of the presence of self-interaction error in current functionals. This error appears because the self-coulomb energy of the electron density is not canceled out by the exchange interaction. Despite several efforts to correct this problem [7–9], self-interaction error remains a significant roadblock for the construction

of more accurate functionals.

Self-interaction error may be ameliorated by using a portion of exact HF exchange in the functional. In the HF method, part of the exchange energy exactly cancels out the self-coulomb energy. As a matter of fact, the success of hybrid methods may be partially attributed to the reduction of self-interaction error by the use of a fixed portion of HF exchange in the functional. Other authors have also proposed a combination of long-range HF exchange with short-range GGA exchange [10].

In this paper, we propose a local hybrid scheme to improve the self-interaction error: our functional resorts to 100% HF exchange in the regions of the density dominated by one-electron-type behavior. We also here assess the performance of such a scheme on a selected group of systems that have shown problems due to self-interaction error when calculated using traditional functionals. Tests of atomization energies in the small G2 set are also included for comparison.

II. THEORY

For a system with one electron, the sum of Coulomb and exchange-correlation energy should be equal to zero. This is the case when the HF method is considered, but is not true for most density functionals. As a result, all currently used exchange functionals include self-interaction error. Using the HF method in connection with a self-interaction free DFT correlation functional fixes the self-interaction error. Unfortunately, the quality of results drops dramatically for molecules [11, 12]. This is in part due to the lack of non-dynamical correlation that is included in the exchange functionals.

In this paper, we define a local hybrid functional where the amount of exact HF and DFT exchange varies according to the local properties of each system, with the variation of the mixing given by a local function, $f(\mathbf{r})$,

*To appear in J. Chem. Phys. **118**, January 15, 2003.

$$E_{XC} = \int d^3\mathbf{r} \rho(\mathbf{r}) [f(\mathbf{r}) e_X^{\text{DFT}}(\mathbf{r}) + (1 - f(\mathbf{r})) e_X^{\text{exact}}(\mathbf{r}) + e_C^{\text{DFT}}(\mathbf{r})] \quad (1)$$

In the formula above, ‘‘DFT’’ stands for regular DFT exchange and correlation, *e.g.*, LSDA or GGA. Exact exchange is introduced in this scheme using the exact exchange energy density that we derive from the definition of the non-local exact exchange energy expression,

$$E_X = \int e_X^{\text{exact}}(\mathbf{r}_1) \rho(\mathbf{r}_1) d^3\mathbf{r}_1 = \frac{1}{2} \int \int \frac{|\rho_1(\mathbf{r}_1, \mathbf{r}_2)|^2}{r_{12}} d^3\mathbf{r}_1 d^3\mathbf{r}_2. \quad (2)$$

An expansion on the atomic basis yields

$$e_X^{\text{exact}}(\mathbf{r}_1) \rho(\mathbf{r}_1) = \frac{1}{2} \sum_{\mu\nu\lambda\kappa} P_{\mu\lambda} P_{\nu\kappa} \chi_\mu(\mathbf{r}_1) \chi_\nu(\mathbf{r}_1) \int d^3\mathbf{r}_2 \frac{\chi_\lambda(\mathbf{r}_2) \chi_\kappa(\mathbf{r}_2)}{|\mathbf{r}_1 - \mathbf{r}_2|}. \quad (3)$$

We have implemented the exact exchange energy density using Eq. (3). However, our results were computed much faster and with similar accuracy using the localized HF (LHF) implementation of Della Sala and Görling [13], which uses a resolution of the identity to simplify Eq. (3) into

$$e_X^{\text{exact}}(\mathbf{r}_1) \rho(\mathbf{r}_1) = \sum_{\mu\nu} Q_{\mu\nu} \chi_\mu(\mathbf{r}_1) \chi_\nu(\mathbf{r}_1), \quad (4)$$

where

$$\mathbf{Q} = \frac{1}{2} \mathbf{S}^{-1} \mathbf{K} \mathbf{P} + \frac{1}{2} \mathbf{P} \mathbf{K} \mathbf{S}^{-1}, \quad (5)$$

where \mathbf{S} , \mathbf{P} , and \mathbf{K} are the overlap, density, and HF exchange matrices, respectively.

The latter is

$$K_{\mu\nu} = \sum_{\sigma\nu} P_{\mu\nu} (\mu\lambda|\sigma\nu). \quad (6)$$

Eq. (4) was utilized for all the calculations reported in this paper.

The expression for the exact exchange energy density can be written in ways different from the one that we have chosen for this work [14]. In principle, any function that integrates to the exact exchange energy can be used. This includes the possibility of adding to the density expression a factor that integrates to zero. In this work, we have chosen not to include a factor like this.

Once the exact exchange density is determined, the next key ingredient for our local hybrid scheme is choosing a local mixing function $f(\mathbf{r})$. This mixing function

determines how much exact exchange and DFT exchange are to be included at each point in space. With self-interaction error in mind, the mixing function that we propose highlights the single orbital dominated regions following Becke’s self-correlation detection function [15]:

$$f(\mathbf{r}) = 1 - \frac{\tau_W}{\tau}, \quad (7)$$

where τ is the kinetic energy density. τ_W is the Weizsäcker kinetic energy density approximation and is defined as follows

$$\tau_W = \frac{|\nabla\rho|^2}{8\rho}. \quad (8)$$

It is important to note that τ_W is exactly equal to τ in one-electron regions, *i.e.*, regions where $\psi \sim e^{-\alpha r}$. Also notice that

$$\tau > 0, \quad (9)$$

$$\tau_W \geq 0, \quad (10)$$

$$\tau \geq \tau_W, \quad (11)$$

and thus

$$0 \leq \frac{\tau_W}{\tau} \leq 1. \quad (12)$$

Substituting Eq. (7) into Eq. (1) we obtain

$$F_{XC} = (1 - \frac{\tau_W}{\tau}) e_X^{\text{DFT}}(\mathbf{r}) + \frac{\tau_W}{\tau} e_X^{\text{exact}}(\mathbf{r}) + e_C^{\text{DFT}}(\mathbf{r}). \quad (13)$$

There will be no self-interaction for one-electron regions where $\tau_W = \tau$ since only exact exchange is used

$$\frac{\tau_W}{\tau} = 1 \Rightarrow F_{XC} = e_X^{\text{local}}(\mathbf{r}) + e_C^{\text{DFT}}(\mathbf{r}). \quad (14)$$

Only DFT exchange will be considered for homogeneous region ($\tau_W = 0$),

$$\frac{\tau_W}{\tau} = 0 \Rightarrow F_{XC} = e_X^{\text{DFT}}(\mathbf{r}) + e_C^{\text{DFT}}(\mathbf{r}). \quad (15)$$

τ_W is equal to zero for uniform densities ($|\nabla\rho|^2 = 0$). Note also that Savin and co-workers [16] have used τ_W as a ‘‘local band gap’’ in recent work. From this viewpoint, our mixing function is such that exact exchange is turned off when the local gap has metallic character.

Local hybrid functionals, as proposed here, belong to the fourth rung on Jacob’s ladder of density functional approximations as proposed by Perdew and Schmidt [12]. When the PBE [17] exchange functional and the PKZB [18] correlation functional are used in Eq. (13), all the

properties for the fourth rung are satisfied. By construction, the exchange energy is set to be self-interaction free for any one-electron density. In the high density limit, such as near the nucleus of an atom, $\tau_W \rightarrow \tau$. Thus, only exact exchange and DFT correlation are used, which is normally believed to be a good approximation for the high-density limit. If we define

$$e_C^{\text{non-dynamic}} = (e_X^{\text{DFT}} - e_X^{\text{exact}}), \quad (16)$$

then local hybrid functionals can be expressed as

$$F_{XC} = e_X^{\text{exact}} + \left(1 - \frac{\tau_W}{\tau}\right) e_C^{\text{non-dynamic}} + e_C^{\text{dynamic}}. \quad (17)$$

From this perspective, our strategy allows for the introduction of position dependent contributions of non-dynamical correlation according to the characteristics of the system under consideration.

III. COMPUTATIONAL METHOD

All calculations were carried out with a development version of the *Gaussian* program suite [19]. DFT calculations in this work were performed using both post-HF and post-LSDA densities.

We have used two different sets of approximate density functionals when testing our local hybrid approach. On one hand, we have used Becke88 exchange [20] with LYP correlation [21], which we call *Lh*-BLYP. On the other hand, we have used PBE exchange with PZKB correlation, which we will refer to as *Lh*-PBEPKZB. Both correlation functionals above include some self-interaction correction. PKZB correlation is self-interaction free in the one-electron regions.

IV. RESULTS AND DISCUSSION

A. Dissociation curves of 2-center 3-electron systems

A set of molecules that has been widely studied to assess the performance of density functionals is the symmetric radical cations A_2^+ [22–27] and their two-center three-electron (2c-3e) bond A-A. Most functionals overestimate the stability of these systems and render equilibrium bond lengths that are too long. These errors originate from self-interactions [24, 26] and, in some cases, from the inclusion of non-dynamic correlation terms when there is none present [23]. The features of this set makes it an ideal candidate to test our local hybrid approach.

Dissociation curves were calculated to study the stability of the two-center three-electron systems (A_2^+). For the sake of clarity, the geometry of each fragment (A)

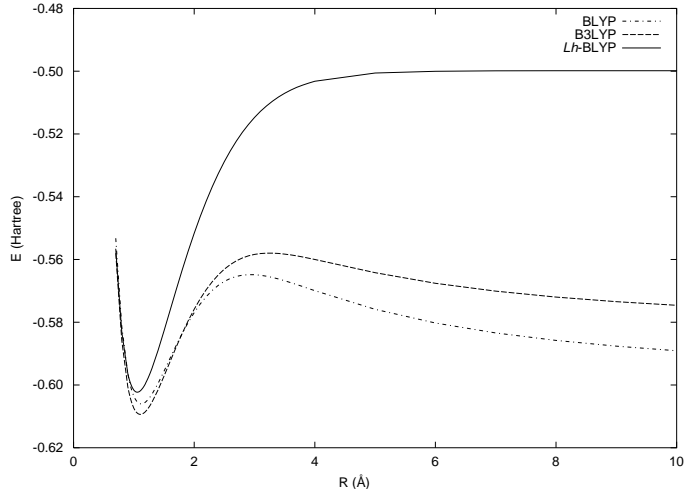


FIG. 1: Dissociation curves for H_2^+ calculated with 6-311G++(3df,3pd) basis set and BLYP, B3LYP, and *Lh*-BLYP functionals.

was kept constant. Only the inter-fragment distance was varied using finite steps of 0.0125 Å to generate potential energy curves. The optimized geometries of the fragments were taken from Gill and Radom [28]. The 6-311G++(3df,3pd) basis set was used for all the 2-center 3-electron calculations.

Figure 1 shows the dissociation curve of H_2^+ for BLYP, B3LYP, and *Lh*-BLYP. In this case since H_2^+ is a one-electron system, by construction, our local hybrid functional coincides with the exact HF curve, regardless of the particular DFT exchange and correlation functional used. Figure 2 presents our results for $(HF)_2^+$ using BLYP, B3LYP, *Lh*-BLYP, and *Lh*-PBEPKZB. It can be seen from this figure how the local hybrid scheme significantly improves the dissociation behavior with respect to BLYP and B3LYP. Similar results were obtained for He_2^+ , Ne_2^+ , Ar_2^+ , $(H_2O)_2^+$, and $(NH_3)_2^+$ but are not displayed for brevity.

Table I presents the calculated equilibrium bond lengths for H_2^+ , He_2^+ , Ne_2^+ , Ar_2^+ , $(HF)_2^+$, $(H_2O)_2^+$, and $(NH_3)_2^+$. All DFT results were obtained using a post-HF procedure. Post-LSDA equilibrium bond lengths are within ~ 0.01 Å of the post-HF results both for regular and local hybrids. As expected, this difference was slightly larger for BLYP. Equilibrium bond lengths are greatly improved for the local hybrid functionals with respect to BLYP, B3LYP, and HF results when compared to experimental data and *ab initio* calculations. On average, local hybrid errors are at least half of the traditional hybrid errors.

Table II shows binding energies calculated for H_2^+ , He_2^+ , Ne_2^+ , Ar_2^+ , $(HF)_2^+$, $(H_2O)_2^+$, and $(NH_3)_2^+$. All DFT results in Table II were calculated using a post-HF procedure. Binding energies were calculated using the separated cation and neutral fragments and the equilibrium structure, as follows

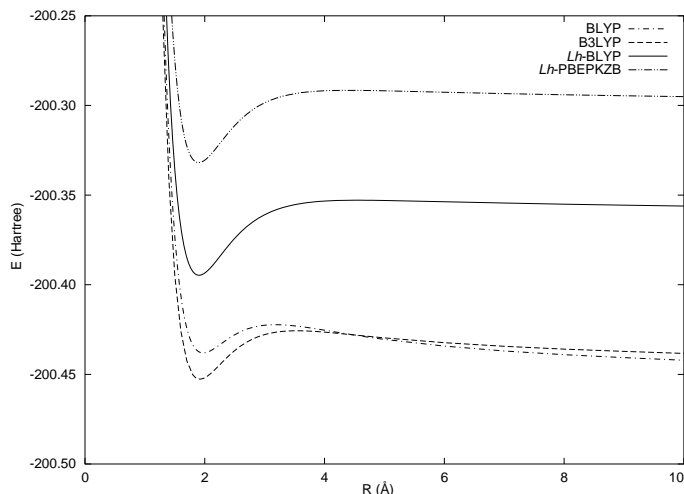


FIG. 2: Dissociation curves for $(\text{HF})_2^+$ calculated with 6-311G++(3df,3pd) basis set and BLYP, B3LYP, *Lh*-BLYP, and *Lh*-PBEPKZB functionals

TABLE I: Equilibrium bond lengths (Å) for the dissociation of two-center three-electron symmetric radical cations.

	H_2^+	He_2^+	Ne_2^+	Ar_2^+	$(\text{HF})_2^+$	$(\text{H}_2\text{O})_2^+$	$(\text{NH}_3)_2^+$
BLYP	1.13	1.16	1.91	2.63	1.98	2.14	2.28
B3LYP	1.11	1.14	1.83	2.54	1.94	2.08	2.23
<i>Lh</i> -BLYP	1.06	1.06	1.79	2.51	1.90	2.08	2.25
<i>Lh</i> -PBEPKZB	1.06	1.06	1.79	2.49	1.90	2.06	2.23
HF	1.06	1.08	1.70	2.44	1.84	2.01	2.20
Exp. ^(a)	1.05	1.08	1.75	2.42	-	-	-
MP2 ^(a)	-	1.09	1.76	2.48	1.88	2.04	2.16

^(a) Reference [22]

$$D_e(\text{A}_2^+) = E(\text{A}) + E(\text{A}^+) - E_{eq}(\text{A}_2^+). \quad (18)$$

No zero-point energy (ZPE) corrections were applied.

The results calculated using a post-LSDA procedure differ from those using a post-HF one, on average, by 1 or 2 kcal/mol both for local and regular hybrids. Again, this difference is slightly larger for BLYP. Local hybrids greatly improve the dissociation energies for the systems under consideration. B3LYP overestimates, on average, the stabilization energies of the A_2^+ type systems by almost 15 kcal/mol and BLYP by almost 20 kcal/mol. In contrast, *Lh*-BLYP overestimates them by 2 kcal/mol on average, and *Lh*-PBEPKZB underestimates them, on average, by 2 kcal/mol. Both functionals yield remarkably consistent results throughout the seven systems. This large and significant improvement for the binding energies is a direct consequence of the functional flexibility to accommodate variable quantities of exact exchange depending on the weight function, which in turn depends

TABLE II: Binding energies (kcal/mol) for two-center three-electron symmetric radical cations.

	H_2^+	He_2^+	Ne_2^+	Ar_2^+	$(\text{HF})_2^+$	$(\text{H}_2\text{O})_2^+$	$(\text{NH}_3)_2^+$
BLYP	68.4	79.8	66.7	45.3	61.3	51.9	51.0
B3LYP	67.4	75.2	55.1	40.7	58.0	47.1	48.5
<i>Lh</i> -BLYP	64.3	54.9	33.9	31.7	38.6	35.5	39.8
<i>Lh</i> -PBEPKZB	64.3	50.3	30.7	30.3	36.2	33.7	38.7
HF	64.3	45.5	3.1	14.4	16.1	18.7	28.6
Exp. ^(a)	61.3	56.9	31.4	29.3	-	-	-
MP4 ^(a)	-	55.3	33.1	28.7	37.4	43.1	37.9

^(a) Reference [22]

on the local position and overall molecular configuration (*i.e.*, the A-A separation).

The amount of exact exchange that the functional employs varies throughout the dissociation curve of each system. To illustrate this issue, we define an average global mixing parameter, a_x , to compare the overall amount of exact exchange that the local hybrid uses for a given system, at a given configuration, with respect to the traditional global hybrids. If we define $E_x^{\text{exact},Lh}$, the exact exchange energy utilized by the local hybrid for a given system as

$$E_x^{\text{exact},Lh} = \int d^3\mathbf{r} \rho(\mathbf{r}) [(1 - f(\mathbf{r})) e_X^{\text{exact}}(\mathbf{r})], \quad (19)$$

and E_x^{HF} , the exact Hartree-Fock exchange for that system, then we define a_x as

$$a_x = \frac{E_x^{\text{exact},Lh}}{E_x^{\text{HF}}} \times 100 \quad (20)$$

Figure 3 shows the change in the average global mixing parameter a_x along the bond dissociation coordinate for Ne_2^+ . At large interatomic distances, the overall amount of exact exchange is larger than at bonding distances. It is worth noting that Ne_2^+ is very well described by the local hybrid in spite of the particularly poor results obtained using BLYP, B3LYP, and HF. In this case, the amount of exact exchange varies from 64 to 67% and is substantially larger than that of B3LYP. Note that even if a_x is in the 20 to 25% interval, the local hybrid may yield significantly different results than the corresponding global hybrid because of the local fluctuations in the amount of exchange inherent to local hybrids.

B. The $\text{H}_2 + \text{H} \rightarrow \text{H} + \text{H}_2$ reaction energy barrier

In order to illustrate the capabilities of the local hybrid scheme, we have calculated the reaction energy barrier

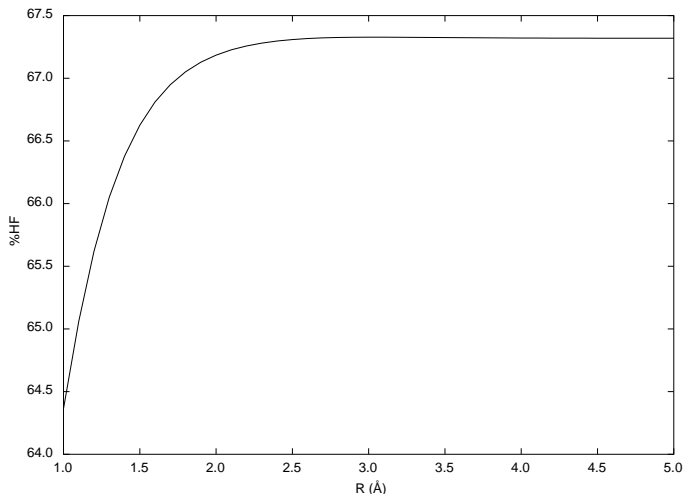


FIG. 3: Average global mixing parameter, a_x , as a function of interatomic distance for Ne_2^+ . This parameter indicates the overall portion of exact exchange that the local hybrid uses for a given system at a given configuration.

TABLE III: Reaction energy barrier (kcal/mol) for the linear hydrogen abstraction $\text{H}_2 + \text{H} \rightarrow \text{H} + \text{H}_2$.

Functional	Energy Barrier ^(a)
HF ^(b)	17.9
BLYP ^(b)	2.9
B3LYP	6.0
<i>Lh</i> -BLYP	10.4
<i>Lh</i> -PBEPKZB	8.9
CCSD(T) ^(b)	9.9
Exp. ^(b)	9.7

^(a)Zero-point energy correction for this reaction is estimated at ~ 1 kcal/mol [29], and should be subtracted from the data tabulated here before comparing to experiment.

^(b)Reference [29]

for a chemical reaction that has traditionally been a difficult case for GGA and hybrid functionals: the simplest hydrogen abstraction, $\text{H}_2 + \text{H} \rightarrow \text{H} + \text{H}_2$. In general, reaction barriers are deemed too low when calculated using GGA or hybrid functionals [29].

Table III presents the classical reaction energy barrier calculated utilizing BLYP, B3LYP, HF, accurate *ab initio* methods, and the local hybrids, and the experimental value. Our DFT calculations for the reaction barrier were carried out using a post-HF procedure with the 6-311G++(3df,3pd) basis set. The geometries of H_2 and the linear transition state were optimized using a gradient minimization of self-consistent HF with the 6-311++G(3df,3pd) basis sets. As with other calculations performed in this work, the post-LSDA results are very close to the post-HF ones (not quoted in Table III).

The reaction energy barrier for the hydrogen abstrac-

TABLE IV: Statistical data for atomization energies (kcal/mol) of the small G2 set (55 molecules). All calculations are carried out using post-HF densities.

	BLYP	B3LYP	<i>Lh</i> -BLYP	<i>Lh</i> -PBEPKZB
MAE ^a	3.9	4.1	19.6	13.0
RMS ^b	5.2	5.6	23.8	17.7
Max (-) dev.	-16.7	-19.5	-59.3	-51.7
Max (+) dev.	6.4	7.5	7.5	7.8

^a Mean absolute error. ^b Root mean square deviation.

tion is significantly improved with the introduction of local hybrids. If we include a ZPE correction of around 1 kcal/mol [29], then the reaction energy barrier calculated with *Lh*-BLYP is within 1 kcal/mol of the experimental value. Results for *Lh*-PBEPKZB are not as accurate as for *Lh*-BLYP but are considerably better than HF, B3LYP, or BLYP. The results for this reaction are very encouraging and show a significant improvement with respect to traditional density functionals.

C. Atomization energies

We have calculated atomization energies for the small G2 set [30] (55 molecules) to assess the performance of the local hybrids. This test is usually performed to gauge the accuracy of new functionals. Equilibrium geometries at the MP2/6-31G* level were used for the 55 molecules. All calculations presented in this section were performed using a post-HF scheme and the 6-311G++(3df,3pd) basis set.

Table IV summarizes the average absolute deviations for the atomization energies of the G2 set. In this particular case, we have compared to the atomization energies calculated by adding ZPE to experimental enthalpies of formation of molecules from gaseous atoms at 0 K. All experimental data were taken from the sources recommended by Curtiss *et al.* [30]. ZPE corrections at the HF/6-31G* level [31] were used in all cases. The fact that we use post-HF densities for all DFT calculations also affects these results. Therefore, it is important to note that the average absolute deviations entries for BLYP and B3LYP in table IV differ from the results presented by other authors [3, 30] and appear higher than expected.

Unfortunately, the local hybrids underperform when compared with BLYP or B3LYP. In general, the local hybrids tend to underestimate the atomization energies. It should be noted that our local hybrids have not been parametrized using experimental data. An examination of the average global mixing parameter, a_x , for the 55 molecule of the set shows that the local hybrid functionals use too much exact exchange, and not enough DFT exchange. Thus, for the G2 set type of molecules the results tend toward exact HF exchange + DFT correlation,

a method known to yield poor thermochemistry.

V. CONCLUSIONS

We have presented a new local hybrid functional scheme with position dependent amounts of exact exchange that partially corrects self-interaction error in exchange functionals. Our method is computationally effective for a wide range of molecular systems. Two-center three-electron symmetric radicals can be modeled accurately with the new scheme both at a qualitative and quantitative level, something that cannot be done accurately with traditional GGA and hybrid functionals. Dissociation energies and equilibrium distances for the 2c-3e systems improve dramatically when calculated using our new local hybrid compared to other functionals. We have

presented an example of a reaction energy barrier with quite remarkable results. Data for atomization energies on the small G2 set is somewhat disappointing compared to the rest of the results presented here. We hope that further exploration of local mixing functions will result in improved results for atomization energies and other properties.

Acknowledgments

The authors thank Sergey Maximoff for useful discussions and Viktor Staroverov for the compilation of the G2 set experimental atomization energies. This work was supported by the National Science Foundation and the Welch Foundation.

-
- [1] R. G. Parr and W. Yang, *Density Functional Theory of Atoms and Molecules* (Oxford University Press, New York, 1989).
- [2] R. E. Stratmann, G. E. Scuseria, and M. J. Frisch, *Chem. Phys. Lett.* **257**, 213 (1996).
- [3] A. D. Becke, *J. Chem. Phys.* **98**, 5648 (1993).
- [4] C. Adamo and V. Barone, *Chem. Phys. Lett.* **274**, 242 (1997).
- [5] G. Orlova and J. D. Goddard, *Mol. Phys.* **100**, 483 (2002).
- [6] J. P. Perdew, M. Ernzerhof, and K. Burke, *J. Chem. Phys.* **105**, 9982 (1996).
- [7] J. P. Perdew and A. Zunger, *Phys. Rev. B* **23**, 5048 (1981).
- [8] H. Chermette, I. Ciofini, F. Mariotti, and C. Daul, *J. Chem. Phys.* **114**, 14467 (2001).
- [9] H. Chermette, I. Ciofini, F. Mariotti, and C. Daul, *J. Chem. Phys.* **115**, 11068 (2001).
- [10] H. Iikura, T. Tsuneda, T. Yanai, and K. Hirao, *J. Chem. Phys.* **115**, 3540 (2001).
- [11] G. E. Scuseria, *J. Chem. Phys.* **97**, 7528 (1992).
- [12] J. P. Perdew and K. Schmidt, in *Density Functional Theory and Its Application to Materials*, edited by V. Van Doren *et al.* (AIP conference proceedings, 2001), p 9.
- [13] F. Della Sala and A. Görling, *J. Chem. Phys.* **115**, 5718 (2001).
- [14] K. Burke, F. G. Cruz, and K. Lam, *J. Chem. Phys.* **109**, 8161 (1998).
- [15] A. D. Becke, *J. Chem. Phys.* **109**, 2092 (1998).
- [16] A. Savin, personal communication.
- [17] J. P. Perdew, M. Ernzerhof, and K. Burke, *Phys. Rev. Lett.* **77**, 3865 (1996).
- [18] J. P. Perdew, S. Kurth, A. Zupan, and P. Blaha, *Phys. Rev. Lett.* **82**, 2544 (1999).
- [19] Gaussian 01, Development Version (Revision B.02) M. J. Frisch, G. W. Trucks, H. B. Schlegel, G. E. Scuseria, M. A. Robb, J. R. Cheeseman, J. A. Montgomery, Jr., T. Vreven, K. N. Kudin, J. C. Burant, S. S. Iyengar, J. M. Millam, J. Tomasi, V. Barone, B. Mennucci, M. Cossi, G. Scalmani, N. Rega, G. A. Petersson, M. Ehara, K. Toyota, M. Hada, R. Fukuda, J. Hasegawa, M. Ishida, T. Nakajima, O. Kitao, H. Nakai, Y. Honda, H. Nakatsuji, X. Li, J. E. Knox, H. P. Hratchian, J. B. Cross, C. Adamo, J. Jaramillo, R. Cammi, C. Pomelli, R. Gomperts, R. E. Stratmann, J. Ochterski, P. Y. Ayala, K. Morokuma, P. Salvador, J. J. Dannenberg, V. G. Zakrzewski, S. Dapprich, A. D. Daniels, M. C. Strain, O. Farkas, D. K. Malick, A. D. Rabuck, K. Raghavachari, J. B. Foresman, J. V. Ortiz, Q. Cui, A. G. Baboul, S. Clifford, J. Cioslowski, B. B. Stefanov, G. Liu, A. Liashenko, P. Piskorz, I. Komaromi, R. L. Martin, D. J. Fox, T. Keith, M. A. Al-Laham, C. Y. Peng, A. Nanayakkara, M. Challacombe, P. M. W. Gill, B. Johnson, W. Chen, M. W. Wong, C. Gonzalez, and J. A. Pople, Gaussian, Inc., Pittsburgh PA, 2002.
- [20] A. D. Becke, *Phys. Rev. A* **38**, 3098 (1988).
- [21] C. Lee, W. Yang, and R. G. Parr, *Phys. Rev. B* **37**, 785 (1988).
- [22] B. Braïda, P. C. Hilbert, and A. Savin, *J. Phys. Chem. A* **102**, 7872 (1998).
- [23] M. Grüning, O. V. Gritsenko, S. J. A. van Gisbergen, and E. J. Baerends, *J. Phys. Chem. A* **105**, 9211 (2001).
- [24] R. Merkle, A. Savin, and H. Preuss, *J. Chem. Phys.* **97**, 9216 (1992).
- [25] M. Sodupe, J. Bertran, L. Rodríguez-Santiago, and E. J. Baerends, *J. Phys. Chem. A* **103**, 166 (1999).
- [26] Y. Zhang and W. Yang, *J. Chem. Phys.* **109**, 2604 (1998).
- [27] T. Bally, and G. N. Sastry, *J. Phys. Chem. A* **101**, 7923 (1997).
- [28] P. W. Gill and L. Radom, *J. Am. Chem. Soc.* **110**, 4931 (1988).
- [29] B. G. Johnson, C. A. Gonzales, P. M. Gill, and J. A. Pople, *Chem. Phys. Lett.* **221**, 100 (1994).
- [30] L. A. Curtiss, K. Raghavachari, P. C. Redfern, and J. A. Pople, *J. Chem. Phys.* **106**, 1063 (1997).
- [31] J. A. Pople, M. Head-Gordon, D. J. Fox, K. Raghavachari, and L. A. Curtiss, *J. Chem. Phys.* **90**, 5622 (1989). L. A. Curtiss, C. Jones, G. W. Trucks, K. Raghavachari, and J. A. Pople, *J. Chem. Phys.* **93**, 2537 (1990).